Int. J. Anal. Appl. (2025), 23:243

International Journal of Analysis and Applications

An Analytical and Numerical Approach to Vegetation–Nutrient Dynamics Involving Symbiotic Nitrogen Fixation and the Allee Effect

Shaher Momani[1,2], Iqbal M. Batiha[2,3,*], Ahmed Bouchenak[4,5], Koichi Unami[6]

[1]*Department of Mathematics, Faculty of Science, University of Jordan, Amman 11942, Jordan*

[2]*Nonlinear Dynamics Research Center (NDRC), Ajman University, Ajman 346, UAE*

[3]*Department of Mathematics, Al Zaytoonah University of Jordan, Amman 11733, Jordan*

[4]*Department of Mathematics, Faculty of Exact Sciences, University Mustapha Stambouli of Mascara, Mascara 29000, Algeria*

[5]*Mathematics Research Center, Near East University, Nicosia 99138, Turkey*

[6]*Graduate School of Agriculture, Kyoto University, Kyoto 606-8502, Japan*

[*]*Corresponding author:* i.batiha@zuj.edu.jo

Abstract. This study develops a nonlinear dynamical system with three variables representing the standardized abundances of a leguminous plant, a non-leguminous plant, and a nutrient resource. The system is governed by a set of nonlinear conformable fractional differential equations without delay. We establish the unique existence of solutions, derive analytical results for special cases, and present a numerical investigation of the agroecological dynamics. The model is grounded in field experiments involving *Trifolium repens* (clover) and *Mentha* × *piperita* (mint) cultivated on both flat and sloped plots. Stable isotope analysis was conducted to semi-quantitatively trace the fate of nitrogen atoms, accounting for isotope fractionation, and to validate the model structure. Leaf area was quantified via image processing, and photometric analysis of soil pore water was used to determine the concentrations of clover, mint, and nitrate-nitrogen. Using repeated least squares estimation, model parameters were calibrated based on observed and normalized variable values. The results indicate a pronounced Allee effect in the interaction between clover and the soil environment.

1. Introduction

In recent years, fractional calculus and conformable operators have attracted significant attention as powerful tools for analyzing complex dynamical systems and developing efficient numerical schemes. Several studies have proposed novel algorithms for solving both linear and

Received: Jul. 5, 2025.

2020 *Mathematics Subject Classification.* 26A33, 34A08, 92B05.

Key words and phrases. conformable derivative; conformable integral; Bernoulli equation; agroecological modeling; nonlinear dynamics; Allee effect; stable isotope.

https://doi.org/10.28924/2291-8639-23-2025-243

ISSN: 2291-8639

nonlinear Volterra integro-differential equations as well as fractional models arising in applied sciences [1–4]. More recently, considerable progress has been made in the analysis of impulsive evolution equations, periodic boundary value problems, and Sturm–Liouville type systems under the conformable framework, establishing existence results, stability conditions, and numerical solutions [5–11]. These contributions highlight the flexibility of conformable fractional derivatives in addressing diverse mathematical problems, thereby motivating their application to ecological and biological models where nonlinear interactions and memory effects play a central role.

In agroecological systems, interactions between plants and nutrient resources play a critical role in determining productivity and ecosystem stability. Mathematical modeling serves as a powerful tool for understanding the complex dynamics among plant species and soil nutrients, particularly in systems that involve both legumes (capable of fixing atmospheric nitrogen) and non-legume plants (which rely on available soil nitrogen). These interactions underpin key ecological processes, including productivity, resilience, and long-term sustainability [12, 13].

Classical differential equation models often fall short in describing biological systems accurately, as they typically overlook memory effects and anomalous transport phenomena observed in processes such as nutrient uptake, root exudation, and plant growth. In contrast, fractional-order models provide a more suitable framework by incorporating long-range temporal dependencies and non-local interactions [14–16].

In this study, we present a nonlinear dynamical model with three variables representing the normalized abundances of a legume (e.g., *Trifolium repens*—white clover), a non-legume (e.g., *Mentha* × *piperita* — peppermint), and a nutrient resource (soil nitrogen) [17]. The system is formulated using conformable fractional differential equations without time delays, enabling a more accurate representation of biological processes characterized by memory and fractional-order dynamics, such as nutrient uptake and plant growth [18–20]. This work makes four key theoretical contributions:

- **Framework Development:** A conformable fractional derivative formulation that generalizes classical agroecological models while preserving mathematical tractability.
- **Analytical Solutions:** Closed-form solutions derived for special cases of the nonlinear system.
- **Numerical Algorithms:** Robust computational schemes for solving the conformable fractional-order model.
- **Stability Analysis:** Detailed characterization of equilibrium states and bifurcation structures.

2. Essential Axioms of Conformable Calculus

In this section, we present the essential properties of the conformable fractional operator, including both its derivative and integral forms, as required for our analysis.

Definition 2.1 ([21]). *Let $f : [0,\infty) \to \mathbb{R}$ be a real-valued function. The* conformable fractional derivative *of f of order $\alpha \in (0,1)$ is defined by*

$$D^{\alpha} f(t) = \lim_{\epsilon \to 0} \frac{f(t+\epsilon t^{1-\alpha}) - f(t)}{\epsilon}, \quad \text{for all } t > 0.$$

We write $D^{\alpha} f(t)$ to denote the conformable derivative of order α. If the conformable fractional derivative exists, we say that f is α-differentiable. *Furthermore, if f is α-differentiable on an interval $(0,a)$ with $a > 0$, and if the limit*

$$\lim_{t \to 0^+} D^{\alpha} f(t)$$

exists, then we define

$$D^{\alpha} f(0) := \lim_{t \to 0^+} D^{\alpha} f(t).$$

This definition coincides with the classical definitions of the Riemann–Liouville and Caputo derivatives when applied to polynomials (up to a constant multiple). One important result is the relationship between the conformable derivative and the classical derivative, as presented in the following theorem:

Theorem 2.1. *Let $\alpha \in (0,1]$, and let f be both α-differentiable and classically differentiable at a point $t > 0$. Then,*

$$D^{\alpha} f(t) = t^{1-\alpha} \frac{d}{dt} f(t).$$

Proof. We apply the definition of the conformable derivative and use the substitution $h = \epsilon t^{1-\alpha}$:

$$\begin{aligned} D^{\alpha} f(t) &= \lim_{\epsilon \to 0} \frac{f(t+\epsilon t^{1-\alpha}) - f(t)}{\epsilon} \\ &= t^{1-\alpha} \lim_{h \to 0} \frac{f(t+h) - f(t)}{h} \\ &= t^{1-\alpha} \frac{d}{dt} f(t). \end{aligned}$$

□

As a consequence of Definition 2.1, the following result holds.

Theorem 2.2. *Let $\alpha \in (0,1]$. If a function $f : [0,\infty) \to \mathbb{R}$ is α-differentiable at $t_0 > 0$, then f is continuous at t_0.*

Proof. By Definition 2.1, since f is α-differentiable at $t_0 > 0$, let $h = \epsilon t_0^{1-\alpha}$. Then the conformable derivative at t_0 can be rewritten as:

$$D^{\alpha} f(t_0) = \lim_{h \to 0} \frac{f(t_0+h) - f(t_0)}{h\, t_0^{\alpha-1}}.$$

Because $D^{\alpha} f(t_0)$ exists and $t_0^{\alpha-1} > 0$, it follows that the numerator must tend to zero as $h \to 0$ in order for the limit to remain finite. That is,

$$\lim_{h \to 0} [f(t_0+h) - f(t_0)] = 0,$$

which implies

$$\lim_{h\to 0} f(t_0+h) = f(t_0).$$

Hence, f is continuous at t_0. □

Although the most important case corresponds to $\alpha \in (0,1)$, one may ask: what if $\alpha \in (n, n+1]$ for some natural number n? The following definition extends the conformable derivative to such cases.

Definition 2.2. *Let $\alpha \in (n, n+1]$, where $n \in \mathbb{N}$, and let f be n-times differentiable at $t > 0$. Then the* conformable fractional derivative *of f of order α is defined by*

$$D^{\alpha} f(t) = \lim_{\epsilon\to 0} \frac{D^{(\lceil\alpha\rceil-1)} f(t+\epsilon t^{\lceil\alpha\rceil-\alpha}) - D^{(\lceil\alpha\rceil-1)} f(t)}{\epsilon},$$

or equivalently,

$$D^{\alpha} f(t) = \lim_{\epsilon\to 0} \frac{D^{(n)} f(t+\epsilon t^{n-\alpha+1}) - D^{(n)} f(t)}{\epsilon},$$

where $\lceil\alpha\rceil$ denotes the smallest integer greater than or equal to α.

Remark 2.1. *As a consequence of Definition 2.2, one can show that*

$$D^{\alpha} f(t) = t^{\lceil\alpha\rceil-\alpha} D^{\lceil\alpha\rceil} f(t) = t^{n-\alpha+1} D^{(n+1)} f(t),$$

where $\alpha \in (n, n+1]$ and f is $(n+1)$-times differentiable at $t > 0$.

One can easily show that D^{α} satisfies the following fundamental properties.

Theorem 2.3. *Let $\alpha \in (0,1]$ and let f, g be α-differentiable at a point $t > 0$. Then:*

(1) *Linearity:* $D^{\alpha}(af+bg) = aD^{\alpha}(f) + bD^{\alpha}(g)$, *for all* $a, b \in \mathbb{R}$.
(2) *Power Rule:* $D^{\alpha}(t^p) = pt^{p-\alpha}$, *for all* $p \in \mathbb{R}$.
(3) *Derivative of a Constant:* $D^{\alpha}(\lambda) = 0$, *for any constant* $\lambda \in \mathbb{R}$.
(4) *Product Rule:* $D^{\alpha}(fg) = gD^{\alpha}(f) + fD^{\alpha}(g)$.
(5) *Quotient Rule:* $D^{\alpha}\left(\frac{f}{g}\right) = \frac{gD^{\alpha}(f) - fD^{\alpha}(g)}{g^2}$, *provided* $g(t) \neq 0$.

Proof. **Proof of the Power Rule.** Using Remark 2.1 and the fact that $D^{\alpha} f(t) = t^{1-\alpha}\frac{d}{dt} f(t)$ when $\alpha \in (0,1]$, we compute:

$$\begin{aligned} D^{\alpha}(t^p) &= t^{1-\alpha}\frac{d}{dt}(t^p) \\ &= t^{1-\alpha}\cdot pt^{p-1} \\ &= pt^{p-\alpha}. \end{aligned}$$

Proof of the Product Rule.

$$\begin{aligned} D^{\alpha}(fg) &= t^{1-\alpha}\frac{d}{dt}(fg) \\ &= t^{1-\alpha}(f'g+fg') \\ &= g(t^{1-\alpha}f') + f(t^{1-\alpha}g') \end{aligned}$$

$$= gD^{\alpha}(f) + fD^{\alpha}(g).$$

□

Remark 2.2. *It is important to note that a function may be α-differentiable at a point without being classically differentiable at that point.*

We now present the definition of the α-fractional integral of a function f, starting from a point $a \geq 0$.

Definition 2.3. *Let $f : [0, \infty) \to \mathbb{R}$ be a real-valued function, and let $\alpha \in (0, 1)$. The* conformable fractional integral *of f of order α starting from a is defined by*

$$I_{\alpha}^{a}(f)(t) = I_{1}^{a}(t^{\alpha-1}f) = \int_{a}^{t} \frac{f(x)}{x^{1-\alpha}}\, dx,$$

where the integral is understood in the usual Riemann sense (possibly improper).

One of the fundamental results is the result stated and proved below.

Theorem 2.4. *Let f be a continuous function on $[a, \infty)$, and let $\alpha \in (0, 1)$. Then, for all $t \geq a$, the conformable fractional derivative of the conformable fractional integral satisfies*

$$D^{\alpha}\left(I_{\alpha}^{a}(f)(t)\right) = f(t).$$

Proof. Since f is continuous on $[a, \infty)$, the integral $I_{\alpha}^{a}(f)(t)$ is differentiable. Then, applying the definition of the conformable derivative, we have:

$$\begin{aligned} D^{\alpha}\left(I_{\alpha}^{a}(f)(t)\right) &= t^{1-\alpha}\frac{d}{dt}\left(\int_{a}^{t} \frac{f(x)}{x^{1-\alpha}}\, dx\right) \\ &= t^{1-\alpha} \cdot \frac{f(t)}{t^{1-\alpha}} \\ &= f(t). \end{aligned}$$

□

The following lemma provides a useful identity relating the conformable integral to the classical derivative.

Lemma 2.1. *Let f be a continuous function defined on $[a, \infty)$, and let $\alpha \in (0, 1)$. Then, for all $t > a$, we have*

$$\frac{d}{dt}\left(I_{\alpha}^{a}(f)(t)\right) = \frac{f(t)}{t^{1-\alpha}}.$$

Proof. Since f is continuous on $[a, \infty)$, the conformable integral $I_{\alpha}^{a}(f)(t)$ is differentiable. From the definition of the conformable derivative:

$$D^{\alpha}\left(I_{\alpha}^{a}(f)(t)\right) = t^{1-\alpha} \cdot \frac{d}{dt}\left(I_{\alpha}^{a}(f)(t)\right).$$

From Theorem 2.4, we know that

$$D^{\alpha}\left(I_{\alpha}^{a}(f)(t)\right) = f(t).$$

Substituting into the equation above gives:

$$t^{1-\alpha} \cdot \frac{d}{dt}\left(I_{\alpha}^{a}(f)(t)\right) = f(t),$$

which implies

$$\frac{d}{dt}\left(I_{\alpha}^{a}(f)(t)\right) = \frac{f(t)}{t^{1-\alpha}}.$$

□

3. On-site Testing and Data Collection

To address the stable isotope analysis of nitrogen and to quantify the natural abundance of ^{15}N, Peoples et al. [22] reported the stable isotope composition using the isotope ratio $\delta^{15}N$ of a sample relative to the atmospheric air standard (expressed in per mill, ‰):

$$\delta^{15}N_{\text{reference}} = \frac{R_{\text{sample}} - R_{\text{standard}}}{R_{\text{standard}}} \times 1000, \tag{3.1}$$

where R_{sample} and R_{standard} denote the molar ratios of $^{15}N/^{14}N$ in the sample and the standard, respectively. By convention, the $\delta^{15}N$ value of atmospheric air is taken as 0.000‰ and is referred to as $\delta^{15}N_{\text{air}}$.

Donahue et al. [23] proposed the following formula to estimate the percentage of nitrogen derived from the atmosphere (%Ndfa) in leguminous plants:

$$\%\text{Ndfa} = \frac{\delta^{15}N_{\text{reference}} - \delta^{15}N_{\text{leg}}}{\delta^{15}N_{\text{reference}} - B} \times 100, \tag{3.2}$$

where $\delta^{15}N_{\text{reference}}$ is the isotopic abundance of a non-legume plant that depends entirely on soil mineral nitrogen, $\delta^{15}N_{\text{leg}}$ is the isotopic abundance in a legume sample, and B is a species-specific constant. Jacot et al. [24] reported $B = -1.66$ for common legume species.

Vinther and Jensen [25] reported that the percentage of nitrogen derived from the atmosphere (%Ndfa) in grass–clover mixtures within grazed organic cropping systems exhibited seasonal variations. Furthermore, Reilly et al. [26] investigated the percentage of nitrogen transferred (%Ntr) from legumes to non-legumes within a mixed quadrat. They proposed the following equation to quantify this transfer:

$$\%\text{Ntr} = \frac{\delta^{15}N_{\text{reference}} - \delta^{15}N_{\text{non-leg}}}{\delta^{15}N_{\text{reference}} - B} \times 100, \tag{3.3}$$

where $\delta^{15}N_{\text{non-leg}}$ is the ^{15}N abundance of the non-leguminous plant sampled from a mixed quadrat that includes legumes.

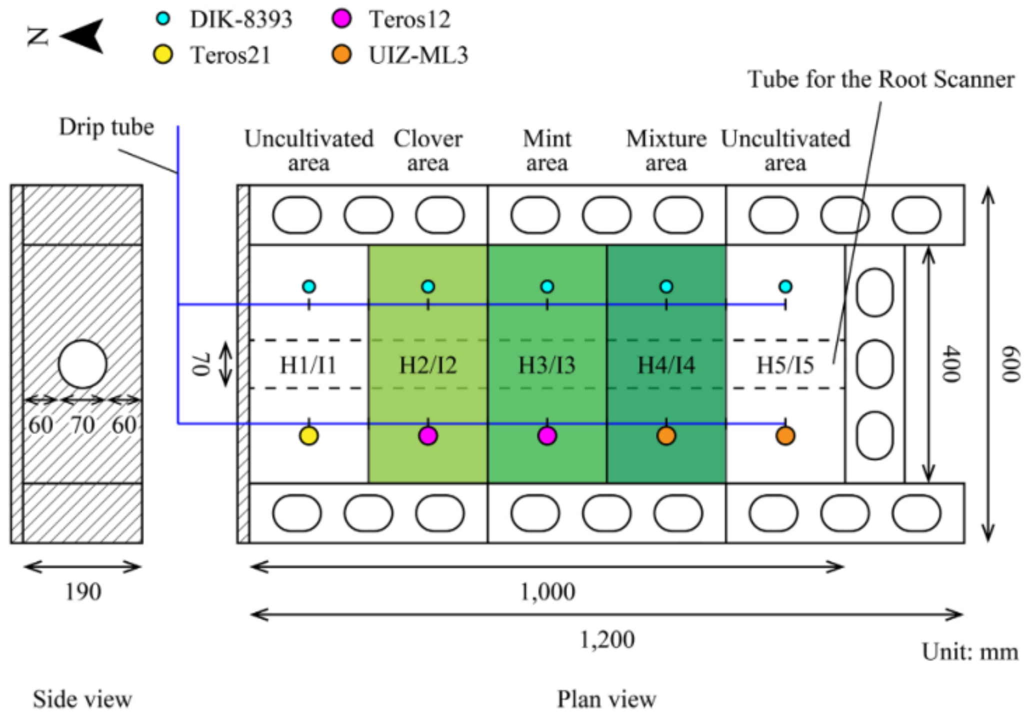

FIGURE 1. Map of the plot setup used in the field experiment [27].

4. Mathematical Investigation of the Model

We hypothesize that the dynamics of the system comprising a leguminous plant (clover), a non-leguminous plant (mint), and a nutrient resource (NO_3-N) can be described by the following system of conformable fractional-order ordinary differential equations:

$$\begin{aligned} D^{\alpha}X &= f_X(X,Y,Z) = a_X f_{ZX} + f_{XX} - \mu_X X, \\ D^{\alpha}Y &= f_Y(X,Y,Z) = a_Y f_{ZY} - \mu_Y Y, \\ D^{\alpha}Z &= f_Z(X,Y,Z) = -f_{ZX} - f_{ZY} + f_{ZZ} - \mu_Z Z, \end{aligned} \tag{4.1}$$

where X, Y, and Z denote the standardized (normalized between 0 and 1) abundances of the leguminous plant, the non-leguminous plant, and the nutrient resource, respectively. The variable t denotes time. The parameters a_X and a_Y are the nutrient absorption coefficients for clover and mint, respectively, while μ_X, μ_Y, and μ_Z represent mortality or decay rates. The functions f_{ZX}, f_{XX}, f_{ZY}, and f_{ZZ} model various nonlinear interactions and are defined as:

$$\begin{aligned} f_{ZX} &= K_X(1-X-Y)Z(\beta_X - Z)X, \\ f_{XX} &= K_S(1-X-Y)(Z+\gamma_X)(\beta_Z - Z)X, \\ f_{ZY} &= K_Y(1-X-Y)Z(\beta_Y - Z)Y, \\ f_{ZZ} &= K_Z Z(1-Z), \end{aligned} \tag{4.2}$$

where K_X, K_S, K_Y, and K_Z are growth rate parameters, and β_X, β_Y, β_Z, and γ_X are shape parameters associated with Allee threshold effects.

Figure 2 conceptually illustrates the agroecological dynamics represented by equations (4.1) and (4.2). The leguminous clover acquires nitrogen through two primary mechanisms: uptake of NO_3-N from soil pore water (modeled by f_{ZX}) and symbiotic nitrogen fixation (SNF) via atmospheric N_2 diffusing into the soil (modeled by f_{XX}). In contrast, the non-leguminous mint solely depends on soil NO_3-N uptake (represented by f_{ZY}). Both plant species are subject to mortality, while the nutrient level Z evolves due to a balance between plant uptake and nitrification of NH_4-N, captured in f_{ZZ}. The total carrying capacity, normalized to 1, imposes geometric constraints on growth through the nonlinear interaction functions.

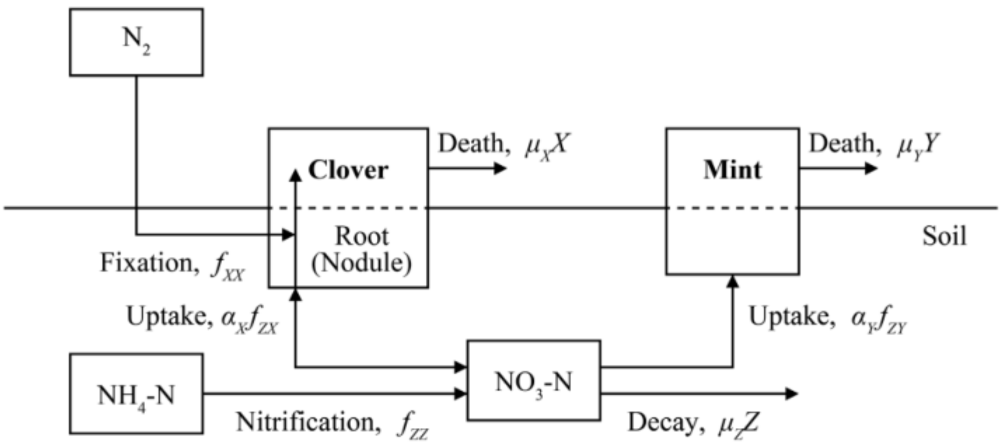

FIGURE 2. Schematic representation of the agroecological model, illustrating interactions among the legume (clover), non-legume (mint), and nutrient resource (NO_3-N) [27].

Remark 4.1. *The structure of the system defined in equations* (4.1)–(4.2) *satisfies the conditions of the Picard–Lindelöf theorem. Therefore, the existence and uniqueness of a local solution to the system are guaranteed.*

4.1. **Physical Interpretation of the Model.** The interaction functions f_{ZX}, f_{XX}, f_{ZY}, and f_{ZZ} respectively represent: nutrient uptake by clover, symbiotic nitrogen fixation (SNF) in clover, nutrient uptake by mint, and nitrogen self-reaction (e.g., nitrification). These interactions are modulated by the total plant abundance: as the combined abundance of clover and mint $(X+Y)$ approaches 1, the overall interaction rates decay due to resource competition and space limitations. Quadratic nonlinearities with respect to the nutrient variable Z introduce potential Allee effects in the dynamics, allowing for threshold-dependent growth or decline. In particular, the terms involving Z in f_{XX} capture the dependence of SNF on environmental nitrogen availability.

The logistic term in f_{ZZ} models the self-dynamics of nitrogen in the soil, where ammonia-N is transformed into nitrate-N (NO_3-N) via nitrification processes. This feedback is key to maintaining nutrient cycling within the system. The physical meanings of all parameters in equations (4.1) and (4.2) are summarized in Table 1. Since X, Y, and Z are normalized between 0 and 1, all rates (including growth and decay) have the dimension of time^{-1}, while shape parameters such as β and γ are dimensionless. In this study, all parameters are assumed to be real-valued.

TABLE 1. Model parameters and their physical interpretations [27]

Parameter	**Description**
a_X	Nitrogen absorption coefficient by clover
a_Y	Nitrogen absorption coefficient by mint
μ_X	Mortality coefficient of clover
μ_Y	Mortality coefficient of mint
μ_Z	Decay coefficient of nitrogen
K_X	Growth rate of clover by nutrient uptake (f_{ZX})
K_S	Growth rate of clover by nitrogen fixation (f_{XX})
K_Y	Growth rate of mint by nutrient uptake (f_{ZY})
K_Z	Growth rate of nitrogen by self-reaction (f_{ZZ})
β_X	Shape parameter for Allee threshold in f_{ZX}
β_Y	Shape parameter for Allee threshold in f_{ZY}
β_Z	First shape parameter for Allee threshold in f_{XX}
γ_X	Second shape parameter for Allee threshold in f_{XX}

4.2. **Analytical Study of the Model.** This part aims to investigate the mathematical properties of the model analytically. By substituting the interaction functions from equation (4.2) into the system (4.1), we obtain the following nonlinear system of conformable fractional ordinary differential equations:

$$\begin{aligned} D^\alpha X &= a_X K_X(1-X-Y)Z(\beta_X - Z)X + K_S(1-X-Y)(Z+\gamma_X)(\beta_Z - Z)X - \mu_X X, \\ D^\alpha Y &= a_Y K_Y(1-X-Y)Z(\beta_Y - Z)Y - \mu_Y Y, \\ D^\alpha Z &= -K_X(1-X-Y)Z(\beta_X - Z)X - K_Y(1-X-Y)Z(\beta_Y - Z)Y + K_Z Z(1-Z) - \mu_Z Z. \end{aligned} \tag{4.3}$$

We begin by invoking the Picard–Lindelöf Theorem, which guarantees the existence and uniqueness of a local solution to the nonlinear system (4.3), provided that the system satisfies the conditions of continuity and Lipschitz continuity with respect to the state variables. Based on this foundational result, we proceed to establish the following propositions concerning the qualitative behavior of the system.

Proposition 4.1. *Consider the nonlinear system of conformable fractional ordinary differential equations* (4.3) *under the following initial conditions:*

$$X(0) = X_0 > 0, \quad Y(0) = 0, \quad Z(0) = 0. \tag{4.4}$$

Then, the system reduces to a nonlinear conformable fractional homogeneous differential equation of Bernoulli type:

$$D^{\alpha}X + (\mu_X - K_S\gamma_X\beta_Z)\,X = -(K_S\gamma_X\beta_Z)X^2. \tag{4.5}$$

For $t \in [0,\infty)$ and $\alpha \in (0,1)$, the equation (4.5) *admits a unique solution, which is given explicitly by:*

$$X(t) = \varphi(t)\,\psi(t) = e^{-I_{\alpha}^{0}(\mu_X - K_S\gamma_X\beta_Z)}\left[-I_{\alpha}^{0}\left(-(K_S\gamma_X\beta_Z)e^{-I_{\alpha}^{0}(\mu_X - K_S\gamma_X\beta_Z)}\right) + \frac{1}{X_0}\right]^{-1}, \tag{4.6}$$

where $\varphi(t)$ denotes the solution to the associated linear homogeneous equation, and $\psi(t)$ corresponds to the transformation component arising from the Bernoulli structure of the nonlinear equation.

Proof. The nonlinear conformable fractional differential equation of Bernoulli type (4.5) can be decomposed into two separate equations. We seek the solution in the form:

$$X(t) = \varphi(t)\psi(t),$$

where $\varphi(t)$ solves the linear component:

$$D^{\alpha}\varphi + (\mu_X - K_S\gamma_X\beta_Z)\varphi = 0,$$

which is a linear conformable first-order ordinary differential equation. Its solution is given by:

$$\varphi(t) = e^{-I_{\alpha}^{0}(\mu_X - K_S\gamma_X\beta_Z)}.$$

Indeed, by using Theorem 2.1, Definition 2.3, and Theorem 2.4, we compute:

$$\begin{aligned}
D^{\alpha}\varphi + (\mu_X - K_S\gamma_X\beta_Z)\varphi &= t^{1-\alpha}\frac{d}{dt}\left(e^{-I_{\alpha}^{0}(\mu_X - K_S\gamma_X\beta_Z)}\right) + (\mu_X - K_S\gamma_X\beta_Z)e^{-I_{\alpha}^{0}(\mu_X - K_S\gamma_X\beta_Z)} \\
&= -t^{1-\alpha}\frac{d}{dt}\left(I_{\alpha}^{0}(\mu_X - K_S\gamma_X\beta_Z)\right)e^{-I_{\alpha}^{0}(\mu_X - K_S\gamma_X\beta_Z)} \\
&\quad + (\mu_X - K_S\gamma_X\beta_Z)e^{-I_{\alpha}^{0}(\mu_X - K_S\gamma_X\beta_Z)} \\
&= -t^{1-\alpha}\cdot\frac{(\mu_X - K_S\gamma_X\beta_Z)}{t^{1-\alpha}}e^{-I_{\alpha}^{0}(\mu_X - K_S\gamma_X\beta_Z)} \\
&\quad + (\mu_X - K_S\gamma_X\beta_Z)e^{-I_{\alpha}^{0}(\mu_X - K_S\gamma_X\beta_Z)} \\
&= -(\mu_X - K_S\gamma_X\beta_Z)e^{-I_{\alpha}^{0}(\mu_X - K_S\gamma_X\beta_Z)} \\
&\quad + (\mu_X - K_S\gamma_X\beta_Z)e^{-I_{\alpha}^{0}(\mu_X - K_S\gamma_X\beta_Z)} = 0.
\end{aligned}$$

The general solution of the truncated Bernoulli equation, excluding the linear component, is represented by the second factor, $\psi(t)$:

$$\varphi D^{\alpha}\psi = -(K_S\gamma_X\beta_Z)\varphi^2\psi^2.$$

Using the known expression $\varphi(t) = e^{-I_{\alpha}^{0}(\mu_X - K_S\gamma_X\beta_Z)}$, we return to the equation for ψ:

$$D^{\alpha}\psi = -(K_S\gamma_X\beta_Z)\varphi\psi^2 \quad\Rightarrow\quad \psi^{-2}D^{\alpha}\psi = -(K_S\gamma_X\beta_Z)e^{-I_{\alpha}^{0}(\mu_X - K_S\gamma_X\beta_Z)}.$$

Since the equation is separable, we integrate both sides:

$$\psi^{-1} = -I_{\alpha}^{0}\left(-(K_S\gamma_X\beta_Z)e^{-I_{\alpha}^{0}(\mu_X - K_S\gamma_X\beta_Z)}\right) + C_0,$$

where C_0 is a constant to be determined using the initial condition (4.4). Taking the reciprocal, we get:

$$\psi(t) = \left[-I_\alpha^0\left(-(K_S\gamma_X\beta_Z)e^{-I_\alpha^0(\mu_X-K_S\gamma_X\beta_Z)}\right)+C_0\right]^{-1}.$$

Thus, the required solution is given by:

$$X(t) = \varphi(t)\psi(t) = e^{-I_\alpha^0(\mu_X-K_S\gamma_X\beta_Z)}\left[-I_\alpha^0\left(-(K_S\gamma_X\beta_Z)e^{-I_\alpha^0(\mu_X-K_S\gamma_X\beta_Z)}\right)+C_0\right]^{-1}.$$

Now, since

$$\begin{aligned} I_\alpha^0(\mu_X-K_S\gamma_X\beta_Z)(t) &= \int_0^t(\mu_X-K_S\gamma_X\beta_Z)\,d_\alpha\xi = \int_0^t(\mu_X-K_S\gamma_X\beta_Z)\,\xi^{\alpha-1}\,d\xi \\ &= (\mu_X-K_S\gamma_X\beta_Z)\int_0^t\xi^{\alpha-1}\,d\xi = (\mu_X-K_S\gamma_X\beta_Z)\left[\frac{\xi^\alpha}{\alpha}\right]_0^t \\ &= (\mu_X-K_S\gamma_X\beta_Z)\cdot\frac{t^\alpha}{\alpha}. \end{aligned}$$

The ICs (4.4) yield the value of the constant C_0 as follows:

$$\begin{aligned} X(0) &= \varphi(0)\psi(0) = e^0\left[-I_\alpha^0\left(-(K_S\gamma_X\beta_Z)(t=0)e^0\right)+C_0\right]^{-1} \\ &= [0+C_0]^{-1} = \frac{1}{C_0} = X_0. \end{aligned}$$

Hence, $C_0 = \frac{1}{X_0}$. Consequently, the solution becomes

$$X(t) = \varphi(t)\psi(t) = e^{-I_\alpha^0(\mu_X-K_S\gamma_X\beta_Z)}\left[-I_\alpha^0\left(-(K_S\gamma_X\beta_Z)e^{-I_\alpha^0(\mu_X-K_S\gamma_X\beta_Z)}\right)+\frac{1}{X_0}\right]^{-1}.$$

To complete the proof, it remains to verify that this solution satisfies Eq. (4.5). Using Theorem 2.1, Definition 2.3, Theorem 2.4, and Lemma 2.1, we compute:

$$\begin{aligned} D^\alpha X(t) &= D^\alpha(\varphi(t)\psi(t)) = \psi(t)D^\alpha\varphi(t)+\varphi(t)D^\alpha\psi(t) \\ &= -\psi(t)(\mu_X-K_S\gamma_X\beta_Z)e^{-I_\alpha^0(\mu_X-K_S\gamma_X\beta_Z)}+\varphi(t)D^\alpha\psi(t) \\ &= -(\mu_X-K_S\gamma_X\beta_Z)\varphi(t)\psi(t)+\varphi(t)D^\alpha\left[\left(-I_\alpha^0\left(-K_S\gamma_X\beta_Z\varphi\right)+\frac{1}{X_0}\right)^{-1}\right] \\ &= -(\mu_X-K_S\gamma_X\beta_Z)X \\ &\quad+\varphi(t)\left[-\left(-I_\alpha^0\left(-K_S\gamma_X\beta_Z\varphi(t)\right)+\frac{1}{X_0}\right)^{-2}D^\alpha\left(-I_\alpha^0\left(-K_S\gamma_X\beta_Z\varphi(t)\right)+\frac{1}{X_0}\right)\right] \\ &= -(\mu_X-K_S\gamma_X\beta_Z)X+\varphi(t)\left[\left(-I_\alpha^0\left(-K_S\gamma_X\beta_Z\varphi(t)\right)+\frac{1}{X_0}\right)^{-2}(K_S\gamma_X\beta_Z)\varphi(t)\right] \\ &= -(\mu_X-K_S\gamma_X\beta_Z)X+\psi^2(t)(K_S\gamma_X\beta_Z)\varphi^2(t) \\ &= -(\mu_X-K_S\gamma_X\beta_Z)X-(K_S\gamma_X\beta_Z)(\varphi(t)\psi(t))^2 \\ &= -(\mu_X-K_S\gamma_X\beta_Z)X-(K_S\gamma_X\beta_Z)X^2. \end{aligned}$$

Hence, the obtained solution satisfies the nonlinear equation (4.5), thereby completing the proof of Proposition 4.1. □

Proposition 4.2. *The nonlinear system of Conformable fractional ordinary differential equations* (4.3) *under the initial conditions:*

$$X(0) = 0, \quad Y(0) = Y_0 > 0, \quad Z(0) = 0, \tag{4.7}$$

reduces to a Conformable fractional homogeneous differential equation of the form:

$$D^\alpha Y + \mu_Y Y = 0. \tag{4.8}$$

Then, for $t \in [0, \infty)$ and $\alpha \in (0, 1)$, there exists a unique solution to (4.8)*, which is explicitly given by:*

$$Y(t) = Y_0 \, e^{-\mu_Y \frac{t^\alpha}{\alpha}}. \tag{4.9}$$

Proof. The general solution to equation (4.8) can be derived using Definition 2.3 as follows:

$$\begin{aligned} Y(t) &= C_1 \, e^{I_\alpha^0(-\mu_Y)} = C_1 \, e^{\int_0^t -\mu_Y \, d_\alpha \xi} \\ &= C_1 \, e^{\int_0^t -\mu_Y \, \xi^{\alpha-1} \, d\xi} = C_1 \, e^{-\mu_Y \left[\frac{\xi^\alpha}{\alpha}\right]_0^t} \\ &= C_1 \, e^{-\mu_Y \frac{t^\alpha}{\alpha}}, \end{aligned}$$

for some constant C_1. Using the initial condition (4.7), we find $C_1 = Y_0$. It remains to verify that the function $Y(t) = Y_0 \, e^{-\mu_Y \frac{t^\alpha}{\alpha}}$ satisfies the differential equation (4.8). Substituting this expression into the left-hand side of the equation and applying the Conformable derivative formula, we obtain:

$$\begin{aligned} D^\alpha Y + \mu_Y Y &= D^\alpha \left(Y_0 \, e^{-\mu_Y \frac{t^\alpha}{\alpha}} \right) + \mu_Y Y_0 \, e^{-\mu_Y \frac{t^\alpha}{\alpha}} \\ &= t^{1-\alpha} \frac{d}{dt} \left(Y_0 \, e^{-\mu_Y \frac{t^\alpha}{\alpha}} \right) + \mu_Y Y_0 \, e^{-\mu_Y \frac{t^\alpha}{\alpha}} \\ &= t^{1-\alpha} \left(-\mu_Y t^{\alpha-1} Y_0 \, e^{-\mu_Y \frac{t^\alpha}{\alpha}} \right) + \mu_Y Y_0 \, e^{-\mu_Y \frac{t^\alpha}{\alpha}} \\ &= -\mu_Y Y_0 \, e^{-\mu_Y \frac{t^\alpha}{\alpha}} + \mu_Y Y_0 \, e^{-\mu_Y \frac{t^\alpha}{\alpha}} \\ &= 0. \end{aligned}$$

Hence, the result follows as required. □

Proposition 4.3. *The nonlinear system of Conformable fractional ordinary differential equations* (4.3) *under the following initial conditions (ICs):*

$$X(0) = 0, \quad Y(0) = 0, \quad Z(0) = Z_0 > 0, \tag{4.10}$$

leads to a nonlinear Conformable fractional differential equation of Bernoulli type, given by:

$$D^\alpha Z + (\mu_Z - K_Z) Z = -K_Z Z^2. \tag{4.11}$$

Then, for $t \in [0, \infty)$ and $\alpha \in (0, 1)$, there exists a smooth unique solution to (4.11)*, which is explicitly given by:*

$$Z(t) = \left[Z_0^{-1} e^{-I_\alpha^0(K_Z - \mu_Z)} + I_\alpha^0 \left(K_Z \, e^{I_\alpha^0(K_Z - \mu_Z)} \right) e^{-I_\alpha^0(K_Z - \mu_Z)} \right]^{-1}. \tag{4.12}$$

Proof. We begin by reducing the nonlinear Conformable fractional differential equation of Bernoulli type, as outlined in the following steps:

Step 1: Divide both sides of equation (4.11) by Z^2:

$$Z^{-2}D^{\alpha}Z + (\mu_Z - K_Z)Z^{-1} = -K_Z.$$

Step 2: Introduce the substitution $\phi = Z^{-1}$ and apply Theorem 2.1. Then, we have

$$\begin{aligned} D^{\alpha}\phi &= t^{1-\alpha}\frac{d}{dt}(\phi) = t^{1-\alpha}\frac{d}{dt}(Z^{-1}) \\ &= t^{1-\alpha}(-1)Z^{-2}\frac{dZ}{dt} = -Z^{-2}\left(t^{1-\alpha}\frac{dZ}{dt}\right) \\ &= -Z^{-2}D^{\alpha}Z. \end{aligned}$$

Thus, we obtain the identity:

$$Z^{-2}D^{\alpha}Z = -D^{\alpha}\phi.$$

Step 3: Substitute this result into the modified equation to get:

$$-D^{\alpha}\phi + (\mu_Z - K_Z)\phi = -K_Z.$$

Step 4: Multiply both sides by (-1) to obtain the standard linear form:

$$D^{\alpha}\phi + (K_Z - \mu_Z)\phi = K_Z, \tag{4.13}$$

which is a first-order linear nonhomogeneous Conformable fractional differential equation. Its solution is given by:

$$\begin{aligned} \phi(t) &= \phi_h(t) + \phi_p(t) \\ &= \phi_0 e^{-I_{\alpha}^{0}(K_Z-\mu_Z)} + I_{\alpha}^{0}\left(K_Z e^{I_{\alpha}^{0}(K_Z-\mu_Z)}\right)e^{-I_{\alpha}^{0}(K_Z-\mu_Z)}, \end{aligned}$$

where ϕ_h and ϕ_p denote the homogeneous and particular solutions, respectively, and ϕ_0 is a constant determined by the initial condition (4.10). We now verify that the homogeneous solution to equation (4.13) is given by

$$\phi_h(t) = \phi_0 e^{-I_{\alpha}^{0}(K_Z-\mu_Z)}.$$

Indeed, we compute:

$$\begin{aligned} D^{\alpha}\phi + (K_Z - \mu_Z)\phi &= \phi_0 t^{1-\alpha}\frac{d}{dt}\left(e^{-I_{\alpha}^{0}(K_Z-\mu_Z)}\right) + (K_Z - \mu_Z)\phi_0 e^{-I_{\alpha}^{0}(K_Z-\mu_Z)} \\ &= -\phi_0 t^{1-\alpha}\frac{d}{dt}\left(I_{\alpha}^{0}(K_Z - \mu_Z)\right)e^{-I_{\alpha}^{0}(K_Z-\mu_Z)} \\ &\quad + (K_Z - \mu_Z)\phi_0 e^{-I_{\alpha}^{0}(K_Z-\mu_Z)} \\ &= -\phi_0 t^{1-\alpha}\cdot\frac{K_Z - \mu_Z}{t^{1-\alpha}}e^{-I_{\alpha}^{0}(K_Z-\mu_Z)} + (K_Z - \mu_Z)\phi_0 e^{-I_{\alpha}^{0}(K_Z-\mu_Z)} \\ &= -(K_Z - \mu_Z)\phi_0 e^{-I_{\alpha}^{0}(K_Z-\mu_Z)} + (K_Z - \mu_Z)\phi_0 e^{-I_{\alpha}^{0}(K_Z-\mu_Z)} = 0. \end{aligned}$$

To obtain the general solution of the conformable differential equation defined by (4.13), we now compute the particular solution:

$$\phi_p(t) = I_\alpha^0\left(K_Z e^{I_\alpha^0(K_Z-\mu_Z)}\right)e^{-I_\alpha^0(K_Z-\mu_Z)}.$$

To complete the proof for this case, we verify that this function satisfies equation (4.13). Substituting the candidate solution into the equation and using Theorem 2.4 and Lemma 2.1, we obtain:

$$\begin{aligned}
D^\alpha\phi_p + (K_Z-\mu_Z)\phi_p &= D^\alpha\left(I_\alpha^0\left(K_Z e^{I_\alpha^0(K_Z-\mu_Z)}\right)e^{-I_\alpha^0(K_Z-\mu_Z)}\right)\\
&\quad + (K_Z-\mu_Z)I_\alpha^0\left(K_Z e^{I_\alpha^0(K_Z-\mu_Z)}\right)e^{-I_\alpha^0(K_Z-\mu_Z)}\\
&= D^\alpha\left(I_\alpha^0\left(K_Z e^{I_\alpha^0(K_Z-\mu_Z)}\right)\right)e^{-I_\alpha^0(K_Z-\mu_Z)}\\
&\quad + I_\alpha^0\left(K_Z e^{I_\alpha^0(K_Z-\mu_Z)}\right)D^\alpha\left(e^{-I_\alpha^0(K_Z-\mu_Z)}\right)\\
&\quad + (K_Z-\mu_Z)I_\alpha^0\left(K_Z e^{I_\alpha^0(K_Z-\mu_Z)}\right)e^{-I_\alpha^0(K_Z-\mu_Z)}.
\end{aligned}$$

Evaluating each term

$$\begin{aligned}
D^\alpha\left(I_\alpha^0\left(K_Z e^{I_\alpha^0(K_Z-\mu_Z)}\right)\right) &= K_Z e^{I_\alpha^0(K_Z-\mu_Z)},\\
D^\alpha\left(e^{-I_\alpha^0(K_Z-\mu_Z)}\right) &= -(K_Z-\mu_Z)e^{-I_\alpha^0(K_Z-\mu_Z)}.
\end{aligned}$$

Substituting back yeilds

$$\begin{aligned}
D^\alpha\phi_p + (K_Z-\mu_Z)\phi_p &= K_Z e^{I_\alpha^0(K_Z-\mu_Z)}e^{-I_\alpha^0(K_Z-\mu_Z)}\\
&\quad - I_\alpha^0\left(K_Z e^{I_\alpha^0(K_Z-\mu_Z)}\right)(K_Z-\mu_Z)e^{-I_\alpha^0(K_Z-\mu_Z)}\\
&\quad + (K_Z-\mu_Z)I_\alpha^0\left(K_Z e^{I_\alpha^0(K_Z-\mu_Z)}\right)e^{-I_\alpha^0(K_Z-\mu_Z)}\\
&= K_Z.
\end{aligned}$$

Hence, the function $\phi_p(t)$ satisfies equation (4.13), confirming its validity. Therefore, the general solution of the conformable differential equation is given by:

$$\begin{aligned}
\phi(t) &= \phi_h(t) + \phi_p(t)\\
&= \phi_0 e^{-I_\alpha^0(K_Z-\mu_Z)} + I_\alpha^0\left(K_Z e^{I_\alpha^0(K_Z-\mu_Z)}\right)e^{-I_\alpha^0(K_Z-\mu_Z)}.
\end{aligned}$$

Now, since $\phi = Z^{-1}$, we conclude that $Z = \phi^{-1}$.

Thus, the solution of the nonlinear Bernoulli-type conformable fractional differential equation (4.11) is given by:

$$Z(t) = \left(\phi_0 e^{-I_\alpha^0(K_Z-\mu_Z)} + I_\alpha^0\left(K_Z e^{I_\alpha^0(K_Z-\mu_Z)}\right)e^{-I_\alpha^0(K_Z-\mu_Z)}\right)^{-1}.$$

Applying the initial conditions (4.10) to determine ϕ_0, we compute:

$$Z(0) = \left(\phi_0 e^0 + I_\alpha^0\left(K_Z e^0\right)e^0\right)^{-1} = \left(\phi_0 + I_\alpha^0(K_Z)\right)^{-1} = \phi_0^{-1} = Z_0.$$

Hence, $\phi_0 = Z_0^{-1}$. Substituting back yields:

$$Z(t) = \left(Z_0^{-1} e^{-I_\alpha^0(K_Z-\mu_Z)} + I_\alpha^0\left(K_Z e^{I_\alpha^0(K_Z-\mu_Z)}\right)e^{-I_\alpha^0(K_Z-\mu_Z)}\right)^{-1}.$$

We now explicitly compute the involved integrals:

$$I^0_\alpha(K_Z-\mu_Z)(t) = \int_0^t (K_Z-\mu_Z)\, d_\alpha\xi = \int_0^t (K_Z-\mu_Z)\xi^{\alpha-1}\, d\xi = (K_Z-\mu_Z)\frac{t^\alpha}{\alpha},$$
$$I^0_\alpha(K_Z)(t) = \int_0^t K_Z\, d_\alpha x = \int_0^t K_Z x^{\alpha-1}\, dx = K_Z\frac{t^\alpha}{\alpha}.$$

This completes the proof of Proposition 4.3. □

4.3. **Numerical Approach.**

4.3.1. *Identification Method for Model Parameters.* **Fate of N and Justification of the Model Structure:** The δ^{15}N-values of the plant samples from the horizontal plot are summarized in Table 2. It is challenging to consistently determine the values of $\delta^{15}N_{\text{reference}}$ required to calculate %Ndfa and %Ntr using equations (3.2) and (3.3). Therefore, we rely exclusively on δ^{15}N-values to infer the fate of nitrogen derived from the atmosphere and its transfer between plant species. Each plant sample collected in Weeks 9 and 12 (vegetative stage) was measured as a whole. In contrast, for Weeks 17 (budding stage) and 20 (flowering stage), the samples were dissected into individual organs—root, stolon, stem, leaf, and flower—for separate measurement. The δ^{15}N-value of the soil, sampled immediately before the experiment's initiation, was 5.217‰, denoted as $\delta^{15}N_{\text{soil}}$. This positive value results from isotope fractionation due to prior agricultural use of the soil.

Values of δ^{15}N between $\delta^{15}N_{\text{air}}$ (defined as 0.000‰) and $\delta^{15}N_{\text{soil}}$ (5.217‰), highlighted in italic in Table 2, suggest that nitrogen in the plant samples originated from symbiotic nitrogen fixation (SNF). However, the inverse is not always valid due to isotope fractionation associated with soil processes such as nitrification, denitrification, root-to-shoot nitrogen transport, and assimilation by the plants [28, 29].

Most of the δ^{15}N-values for clover from plot H2 (except those from the flower and leaf in Week 20) strongly indicate active SNF, supporting the presence of f_{XX}. Conversely, δ^{15}N-values for mint from plot H3 confirm the absence of SNF, with the exception of root samples from Week 17 ($\delta^{15}N = 1.340$), which is less than $\delta^{15}N_{\text{soil}}$. Compared to H3, mint in H4 showed a greater number of δ^{15}N-values below $\delta^{15}N_{\text{soil}}$, suggesting that nitrogen fixed by clover was transferred to the soil (negative f_{ZX}), then absorbed by mint (positive f_{ZY}). This hypothesis is supported by the observation of clover stolons from H2 spreading into H3 as early as Week 10, likely facilitating such nitrogen transfer, as evidenced by the Week 17 root value. To statistically confirm isotope fractionation between the budding and flowering stages, one-sided Mann–Whitney U tests [30] were conducted. The p-values for testing the null hypothesis of identical δ^{15}N distributions between Week 17 and Week 20 were:

- 0.0556 for clover from H2,
- 0.1143 for mint from H3,
- 0.0357 for clover from H4, and
- 0.0556 for mint from H4.

Significant increases in δ^{15}N from Week 17 to Week 20 were observed in the roots of both clover and mint in H4. Root imagery revealed that plant roots experienced the most development during this period, implying that the increases in δ^{15}N were due to isotope fractionation within the biomass, including within the root tissues themselves.

TABLE 2. δ^{15}N-values (‰) of plant samples from the horizontal plot. Italic values indicate estimates between $\delta^{15}N_{air}$ (0.000‰) and $\delta^{15}N_{soil}$ (5.217‰) [27].

Week	**Part**	**Clover (H2)**	**Mint (H3)**	**Clover (H4)**	**Mint (H4)**
9	Whole	*3.754*	6.606	6.040	*
12	Whole	*1.715*	6.773	*4.168*	6.761
17	Leaf	*1.573*	*5.332*	*2.122*	*4.800*
	Stem	*0.684*	6.104	*1.040*	*4.591*
	Stolon	*1.639*	*	*	*2.077*
	Root	*1.638*	*1.340*	*0.786*	*0.896*
20	Flower	8.336	*5.172*	*5.258*	10.615
	Leaf	7.815	25.042	*6.443*	*7.370*
	Stem	*1.054*	16.488	8.262	*1.798*
	Stolon	*3.140*	27.378	*1.976*	*5.812*
	Root	*2.480*	**	9.278	8.116

Note: Italicized entries lie between $\delta^{15}N_{air} = 0.000‰$ and $\delta^{15}N_{soil} = 5.217‰$.
* Not measured due to sample limitation. ** Measurement failed due to technical error.

Keys:
* The sample was too small to measure.
** Instrument malfunction, possibly due to incomplete combustion of the sample.

Data of NO_3-N in Soil Pore Water and Leaf Area (LA) for Model Parameter Identification:
The identification method developed previously was applied to the observed and standardized data from plots H1, H2, H3, and H5 to estimate the parameter values listed in Table 3. The values of Y from H4 were too low to support parameter identification; therefore, the dynamics of X, Y, and Z in H4 are reserved for model validation purposes.

TABLE 3. Identified parameter values for different models based on experimental setups [27].

Parameter	Identified Value		
	From HeZdZ	From H3YZdZ	From H2XYdZ
a_X		1.168	
a_Y		0.128 (H3YZdY), 0.171 (H3YZdY0)	
μ_X		0.532	
μ_Y		−0.110 (H3YZdY), 0.000 (H3YZdY0)	
μ_Z	0.367	0.108	3.799
K_X		−24.133	
K_S		1.365	
K_Y		3.127	
K_Z	0.849	2.248	5.237
β_X		0.169	
β_Y		3.887	
β_Z		0.234	
γ_X		6.371	

4.3.2. *Visualization.* The general solution of the nonlinear agroecological system (4.3) under the initial conditions (4.5) is expressed as:

$$X(t) = \varphi(t)\,\psi(t) = e^{-I_\alpha^0(\mu_X - K_S\gamma_X\beta_Z)} \left[-I_\alpha^0\left(-(K_S\gamma_X\beta_Z)\, e^{-I_\alpha^0(\mu_X - K_S\gamma_X\beta_Z)} \right) + \frac{1}{X_0} \right]^{-1}.$$

For enhanced visualization and numerical computation, we now simplify each term.

Step 1: Exponential Term.

$$\begin{aligned} e^{-I_\alpha^0(\mu_X - K_S\gamma_X\beta_Z)(t)} &= e^{-\int_0^t (\mu_X - K_S\gamma_X\beta_Z)\, d_\alpha \xi} = e^{-\int_0^t (\mu_X - K_S\gamma_X\beta_Z)\, \xi^{\alpha-1} d\xi} \\ &= e^{-(\mu_X - K_S\gamma_X\beta_Z)\frac{t^\alpha}{\alpha}}. \end{aligned}$$

Step 2: Fractional Integral Term.

$$\begin{aligned} -I_\alpha^0\left(-(K_S\gamma_X\beta_Z)\, e^{-I_\alpha^0(\mu_X - K_S\gamma_X\beta_Z)} \right)(t) &= (K_S\gamma_X\beta_Z)\, I_\alpha^0\left(e^{-I_\alpha^0(\mu_X - K_S\gamma_X\beta_Z)} \right) \\ &= (K_S\gamma_X\beta_Z) \int_0^t e^{-(\mu_X - K_S\gamma_X\beta_Z)\frac{x^\alpha}{\alpha}}\, x^{\alpha-1} dx \\ &= \frac{K_S\gamma_X\beta_Z}{K_S\gamma_X\beta_Z - \mu_X} \left(e^{-(\mu_X - K_S\gamma_X\beta_Z)\frac{t^\alpha}{\alpha}} - 1 \right). \end{aligned}$$

Final Expression. Substituting the above results into the expression for $X(t)$, we obtain:

$$X(t) = e^{-(\mu_X - K_S\gamma_X\beta_Z)\frac{t^\alpha}{\alpha}} \left[\frac{K_S\gamma_X\beta_Z}{K_S\gamma_X\beta_Z - \mu_X} \left(e^{-(\mu_X - K_S\gamma_X\beta_Z)\frac{t^\alpha}{\alpha}} - 1 \right) + \frac{1}{X_0} \right]^{-1}. \tag{4.14}$$

This closed-form solution facilitates efficient simulation and plotting of $X(t)$ for given parameters and initial conditions.

TABLE 4. Closed-form solutions of the nonlinear agroecological system (4.3) under ICs (4.4), computed for fractional orders $\alpha = 1, \frac{1}{4}, \frac{1}{2}$, and $\frac{3}{4}$ using parameter values from the H3YZdZ dataset.

X_0	α	μ_X	K_S	γ_X	β_Z	$X(t)$
1	1	0.532	1.365	6.371	0.234	$e^{1.50296111t}\left[\frac{2.03496111}{1.50296111}\left(e^{1.50296111t}-1\right)+1\right]^{-1}$
1	$\frac{1}{4}$	0.532	1.365	6.371	0.234	$e^{1.50296111\frac{t^{1/4}}{1/4}}\left[\frac{2.03496111}{1.50296111}\left(e^{1.50296111\frac{t^{1/4}}{1/4}}-1\right)+1\right]^{-1}$
1	$\frac{1}{2}$	0.532	1.365	6.371	0.234	$e^{1.50296111\frac{t^{1/2}}{1/2}}\left[\frac{2.03496111}{1.50296111}\left(e^{1.50296111\frac{t^{1/2}}{1/2}}-1\right)+1\right]^{-1}$
1	$\frac{3}{4}$	0.532	1.365	6.371	0.234	$e^{1.50296111\frac{t^{3/4}}{3/4}}\left[\frac{2.03496111}{1.50296111}\left(e^{1.50296111\frac{t^{3/4}}{3/4}}-1\right)+1\right]^{-1}$

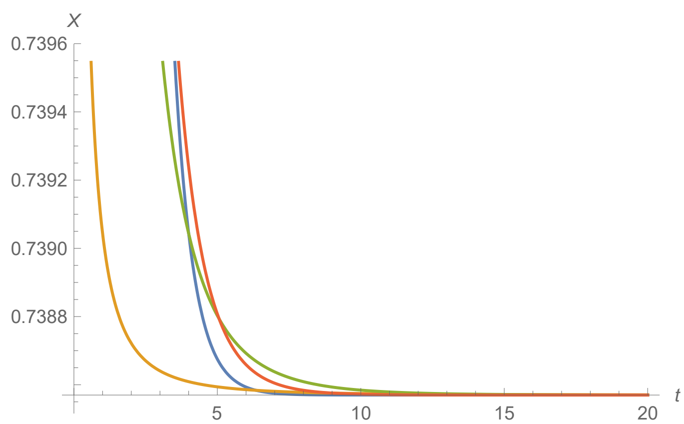

FIGURE 3. Behavior of the solution $X(t)$ with parameter values μ_X, K_S, γ_X, and β_Z taken from H3YZdZ under integer and fractional orders $\alpha = \left(1, \frac{1}{4}, \frac{1}{2}, \frac{3}{4}\right)$.

The general solution of the nonlinear agroecological system (4.3) under the initial conditions (4.4) is given by:

$$Y(t) = Y_0 e^{-\mu_Y \frac{t^\alpha}{\alpha}}, \tag{4.15}$$

where Y_0 is the initial value of Y, μ_Y is the mortality rate, and α denotes the order of the conformable fractional derivative.

TABLE 5. Solutions of the nonlinear agroecological system (4.3) under ICs (4.7) using μ_Y values from H3YZdY and H3YZdY0, for various orders $\alpha = 1, \frac{1}{4}, \frac{1}{2}, \frac{3}{4}$.

Y_0	α	μ_Y (from H3YZdY)	$Y(t)$	μ_Y (from H3YZdY0)	$Y(t)$
1	1	−0.110	$e^{0.110\,t}$	0.000	1
1	$\frac{1}{4}$	−0.110	$e^{0.440\,t^{1/4}}$	0.000	1
1	$\frac{1}{2}$	−0.110	$e^{0.220\,t^{1/2}}$	0.000	1
1	$\frac{3}{4}$	−0.110	$e^{\frac{0.110}{0.75}\,t^{3/4}}$	0.000	1

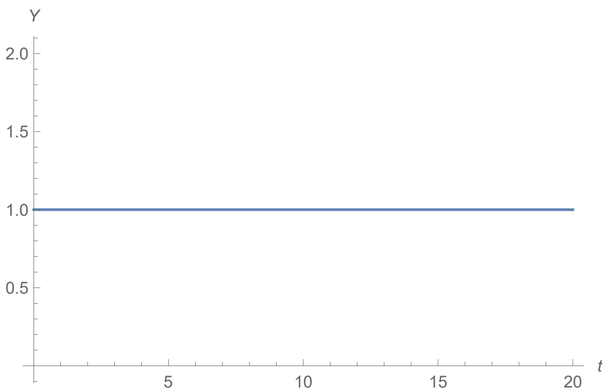

(A) $Y(t)$ with μ_Y from H3YZdY0

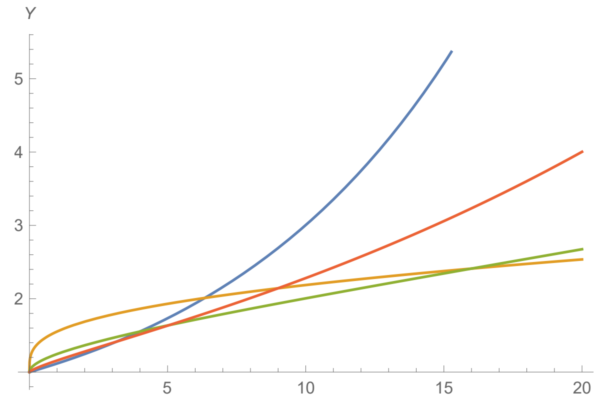

(B) $Y(t)$ with μ_Y from H3YZdY

FIGURE 4. The behavior of the solution $Y(t)$ using μ_Y from H3YZdY and H3YZdY0 under integer and fractional orders $\alpha \in \left\{1, \frac{1}{4}, \frac{1}{2}, \frac{3}{4}\right\}$.

The general solution of the nonlinear agroecological system (4.3) under the initial conditions (4.10) is given by:

$$Z(t) = \left(\frac{1}{Z_0} e^{-I_\alpha^0 (K_Z - \mu_Z)} + I_\alpha^0 \left(K_Z e^{I_\alpha^0 (K_Z - \mu_Z)}\right) e^{-I_\alpha^0 (K_Z - \mu_Z)}\right)^{-1}.$$

Since

$$\begin{aligned} e^{-I_\alpha^0 (K_Z - \mu_Z)(t)} &= e^{-\int_0^t (K_Z - \mu_Z)\, d_\alpha \xi} = e^{-\int_0^t (K_Z - \mu_Z)\, \xi^{\alpha-1} d\xi} \\ &= e^{-\left[(K_Z - \mu_Z) \frac{\xi^\alpha}{\alpha}\right]_0^t} = e^{-(K_Z - \mu_Z)\frac{t^\alpha}{\alpha}}, \end{aligned}$$

and

$$\begin{aligned} I_\alpha^0 \left(K_Z e^{I_\alpha^0 (K_Z - \mu_Z)}\right)(t) &= K_Z \cdot I_\alpha^0 \left(e^{I_\alpha^0 (K_Z - \mu_Z)}\right) \\ &= K_Z \int_0^t e^{\int_0^x (K_Z - \mu_Z)\, d_\alpha \xi}\, d_\alpha x \\ &= K_Z \int_0^t e^{(K_Z - \mu_Z)\frac{x^\alpha}{\alpha}}\, x^{\alpha-1} dx \\ &= \frac{K_Z}{K_Z - \mu_Z} \left[e^{(K_Z - \mu_Z)\frac{x^\alpha}{\alpha}}\right]_0^t \\ &= \frac{K_Z}{K_Z - \mu_Z} \left(e^{(K_Z - \mu_Z)\frac{t^\alpha}{\alpha}} - 1\right). \end{aligned}$$

Consequently, the solution becomes

$$Z(t) = \left(\frac{1}{Z_0} e^{-(K_Z - \mu_Z)\frac{t^\alpha}{\alpha}} + \left(\frac{K_Z}{K_Z - \mu_Z}\left(e^{(K_Z - \mu_Z)\frac{t^\alpha}{\alpha}} - 1\right)\right) e^{-(K_Z - \mu_Z)\frac{t^\alpha}{\alpha}}\right)^{-1}. \tag{4.16}$$

TABLE 6. Solution of the nonlinear agroecological system (4.3) under ICs (4.10) with K_Z and μ_Z from HeZdZ, subject to integer and fractional orders $\alpha = 1, \frac{1}{4}, \frac{1}{2}, \frac{3}{4}$.

Z_0	α	μ_Z (HeZdZ)	K_Z (HeZdZ)	$Z(t)$
1	1	0.367	0.849	$\left(e^{-0.482t} + \left(\frac{0.849}{0.482}\left(e^{0.482t} - 1\right)\right) e^{-0.482t}\right)^{-1}$
1	$\frac{1}{4}$	0.367	0.849	$\left(e^{-0.482\frac{t^{\frac{1}{4}}}{\frac{1}{4}}} + \left(\frac{0.849}{0.482}\left(e^{0.482\frac{t^{\frac{1}{4}}}{\frac{1}{4}}} - 1\right)\right) e^{-0.482\frac{t^{\frac{1}{4}}}{\frac{1}{4}}}\right)^{-1}$
1	$\frac{1}{2}$	0.367	0.849	$\left(e^{-0.482\frac{t^{\frac{1}{2}}}{\frac{1}{2}}} + \left(\frac{0.849}{0.482}\left(e^{0.482\frac{t^{\frac{1}{2}}}{\frac{1}{2}}} - 1\right)\right) e^{-0.482\frac{t^{\frac{1}{2}}}{\frac{1}{2}}}\right)^{-1}$
1	$\frac{3}{4}$	0.367	0.849	$\left(e^{-0.482\frac{t^{\frac{3}{4}}}{\frac{3}{4}}} + \left(\frac{0.849}{0.482}\left(e^{0.482\frac{t^{\frac{3}{4}}}{\frac{3}{4}}} - 1\right)\right) e^{-0.482\frac{t^{\frac{3}{4}}}{\frac{3}{4}}}\right)^{-1}$

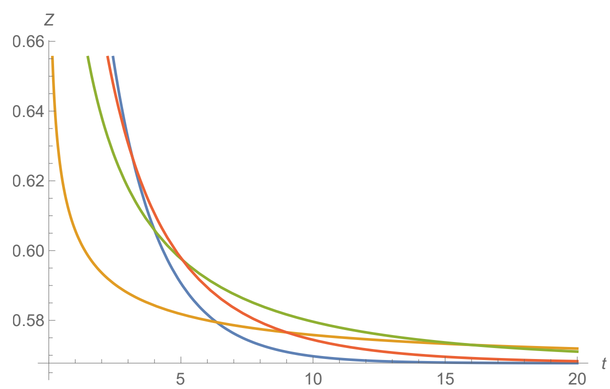

FIGURE 5. The behavior of the solution $Z(t)$ with μ_Z and K_Z from HeZdZ, subject to the integer and fractional orders $\alpha = \left(1, \frac{1}{4}, \frac{1}{2}, \frac{3}{4}\right)$.

TABLE 7. Solution of the nonlinear agroecological system (4.3) under ICs (4.10) with K_Z and μ_Z identified from H3YZdZ, subject to integer and fractional orders $\alpha = 1, \frac{1}{4}, \frac{1}{2}, \frac{3}{4}$.

Z_0	α	μ_Z from H3YZdZ	K_Z from H3YZdZ	$Z(t)$
1	1	0.108	2.248	$\left(e^{-2.14t} + \left(\frac{2.248}{2.14}\left(e^{2.14t} - 1\right)\right) e^{-2.14t}\right)^{-1}$
1	$\frac{1}{4}$	0.108	2.248	$\left(e^{-2.14\frac{t^{\frac{1}{4}}}{\frac{1}{4}}} + \left(\frac{2.248}{2.14}\left(e^{2.14\frac{t^{\frac{1}{4}}}{\frac{1}{4}}} - 1\right)\right) e^{-2.14\frac{t^{\frac{1}{4}}}{\frac{1}{4}}}\right)^{-1}$
1	$\frac{1}{2}$	0.108	2.248	$\left(e^{-2.14\frac{t^{\frac{1}{2}}}{\frac{1}{2}}} + \left(\frac{2.248}{2.14}\left(e^{2.14\frac{t^{\frac{1}{2}}}{\frac{1}{2}}} - 1\right)\right) e^{-2.14\frac{t^{\frac{1}{2}}}{\frac{1}{2}}}\right)^{-1}$
1	$\frac{3}{4}$	0.108	2.248	$\left(e^{-2.14\frac{t^{\frac{3}{4}}}{\frac{3}{4}}} + \left(\frac{2.248}{2.14}\left(e^{2.14\frac{t^{\frac{3}{4}}}{\frac{3}{4}}} - 1\right)\right) e^{-2.14\frac{t^{\frac{3}{4}}}{\frac{3}{4}}}\right)^{-1}$

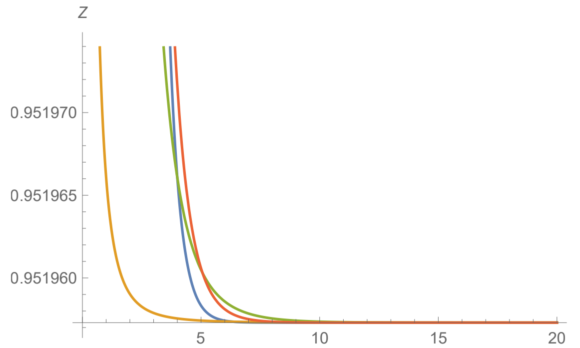

FIGURE 6. Behavior of the solution $Z(t)$ with μ_Z and K_Z from H3YZdZ, subject to integer and fractional orders $\alpha = \left(1, \frac{1}{4}, \frac{1}{2}, \frac{3}{4}\right)$.

TABLE 8. Solution of the nonlinear agroecological system (4.3) under ICs (4.10) with K_Z and μ_Z identified from H2XYdZ, subject to the integer and fractional order $\alpha = 1, \frac{1}{4}, \frac{1}{2}, \frac{3}{4}$.

Z_0	α	μ_Z from H2XYdZ	K_Z from H2XYdZ	$Z(t)$
1	1	3.799	5.237	$\left(e^{-1.438t} + \left(\frac{5.237}{1.438}\left(e^{1.438t} - 1\right)\right)e^{-1.438t}\right)^{-1}$
1	$\frac{1}{4}$	3.799	5.237	$\left(e^{-1.438\frac{t^{\frac{1}{4}}}{\frac{1}{4}}} + \left(\frac{5.237}{1.438}\left(e^{1.438\frac{t^{\frac{1}{4}}}{\frac{1}{4}}} - 1\right)\right)e^{-1.438\frac{t^{\frac{1}{4}}}{\frac{1}{4}}}\right)^{-1}$
1	$\frac{1}{2}$	3.799	5.237	$\left(e^{-1.438\frac{t^{\frac{1}{2}}}{\frac{1}{2}}} + \left(\frac{5.237}{1.438}\left(e^{1.438\frac{t^{\frac{1}{2}}}{\frac{1}{2}}} - 1\right)\right)e^{-1.438\frac{t^{\frac{1}{2}}}{\frac{1}{2}}}\right)^{-1}$
1	$\frac{3}{4}$	3.799	5.237	$\left(e^{-1.438\frac{t^{\frac{3}{4}}}{\frac{3}{4}}} + \left(\frac{5.237}{1.438}\left(e^{1.438\frac{t^{\frac{3}{4}}}{\frac{3}{4}}} - 1\right)\right)e^{-1.438\frac{t^{\frac{3}{4}}}{\frac{3}{4}}}\right)^{-1}$

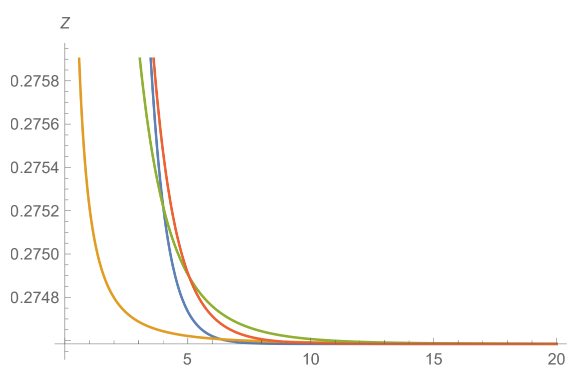

FIGURE 7. The behavior of solution $Z(t)$ with μ_Z and K_Z from H2XYdZ subject to the integer and fractional orders $\alpha = \left(1, \frac{1}{4}, \frac{1}{2}, \frac{3}{4}\right)$.

The asymptotic behavior of the agroecological system (4.3) takes the following forms, depending on the identified values of the parameters from HeZdZ, H3YZdZ, and H2XYdZ. It also depends on whether the system is of integer or fractional order α.

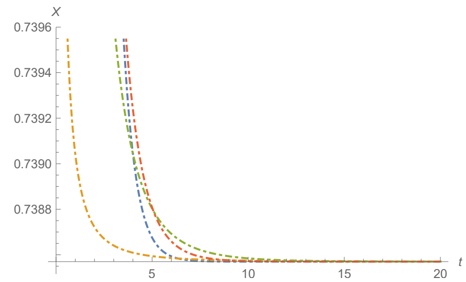

(A) $X(t)$

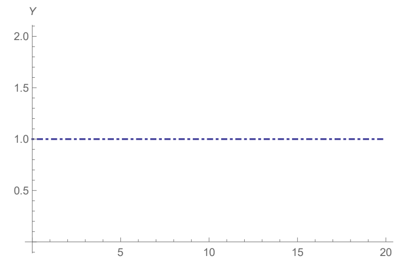

(B) $Y(t)$

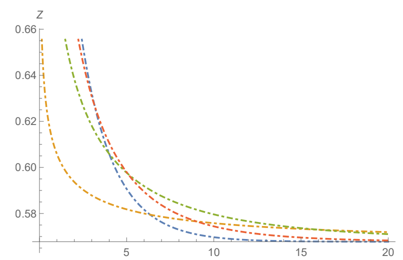

(C) $Z(t)$

FIGURE 8. Asymptotic behavior of the agroecological system with μ_X, K_S, γ_X, and β_Z from H3YZdZ; μ_Y from H3YZdY0; and μ_Z and K_Z from HeZdZ.

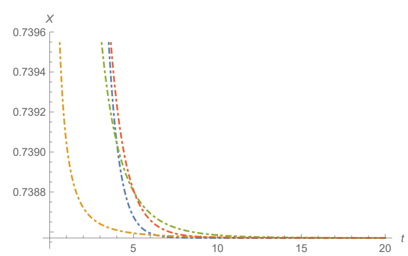

(A) $X(t)$

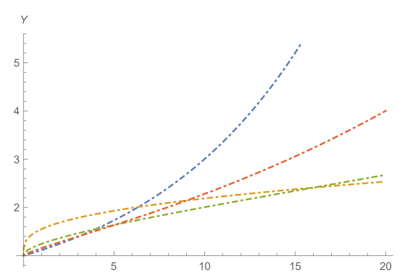

(B) $Y(t)$

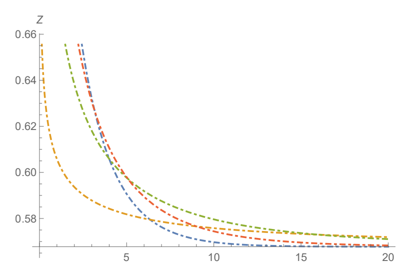

(C) $Z(t)$

FIGURE 9. Asymptotic behavior of the agroecological system with μ_X, K_S, γ_X, and β_Z from H3YZdZ; μ_Y from H3YZdY; and μ_Z and K_Z from HeZdZ.

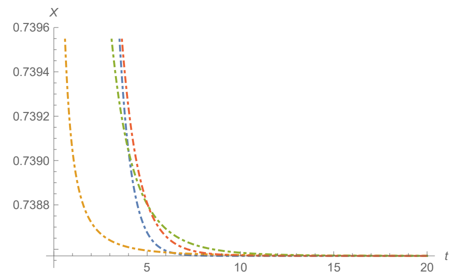

(A) $X(t)$

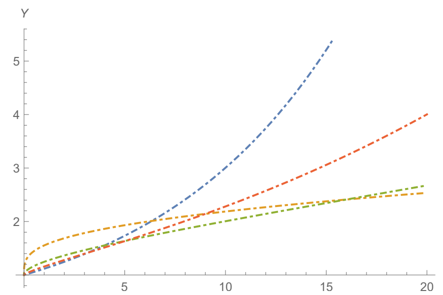

(B) $Y(t)$

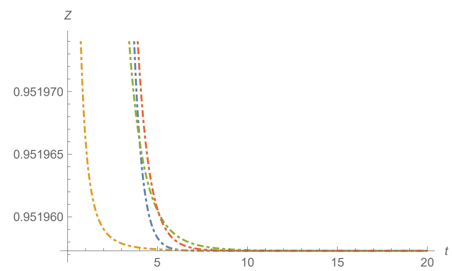

(C) $Z(t)$

FIGURE 10. Asymptotic behavior of the agroecological system, with μ_X, K_S, γ_X, and β_Z from H3YZdZ; μ_Y from H3YZdY; and μ_Z and K_Z from H3YZdZ.

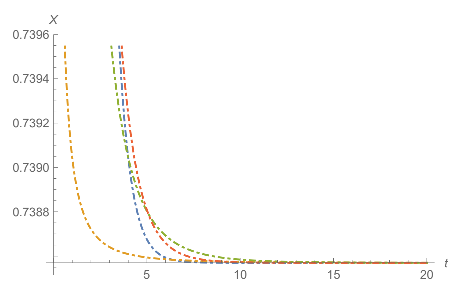

(A) $X(t)$

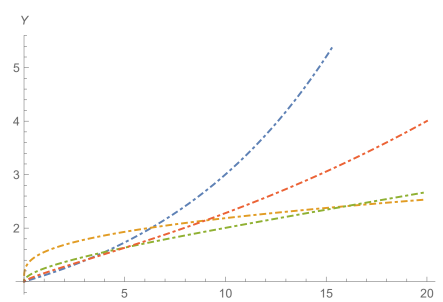

(B) $Y(t)$

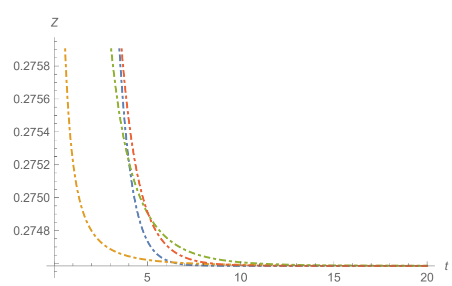

(C) $Z(t)$

FIGURE 11. Asymptotic behavior of the agroecological system, with μ_X, K_S, γ_X, and β_Z from H3YZdZ; μ_Y from H3YZdY; and μ_Z and K_Z from H2XYdZ.

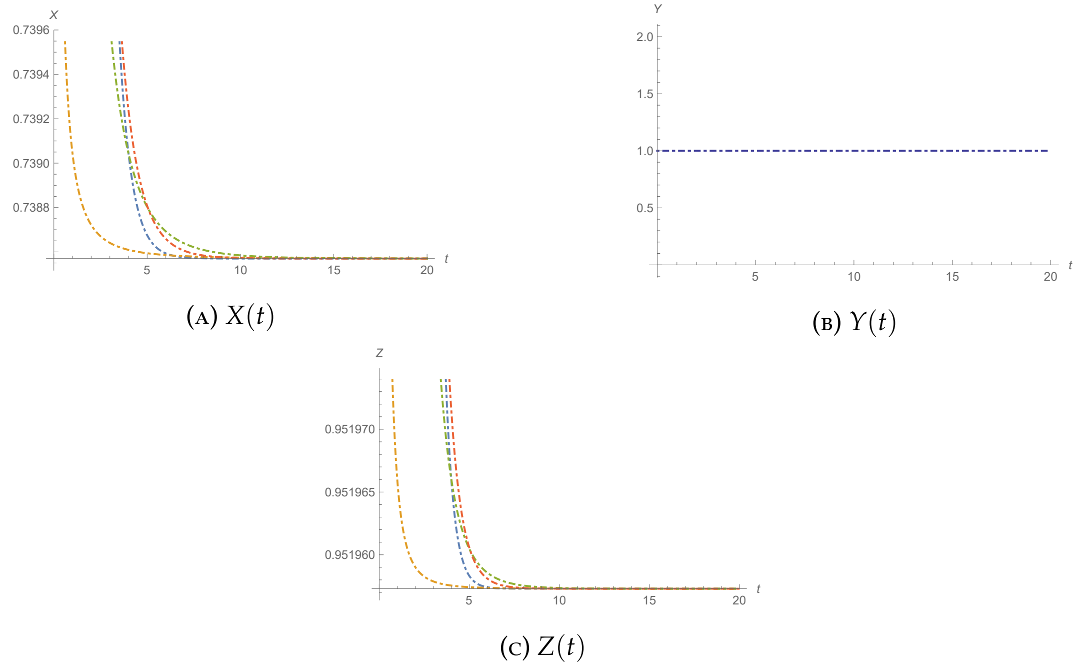

(A) $X(t)$ (B) $Y(t)$

(C) $Z(t)$

Figure 12. Asymptotic behavior of the agroecological system with μ_X, K_S, γ_X, and β_Z from H3YZdZ; μ_Y from H3YZdY0; and μ_Z and K_Z from H3YZdZ.

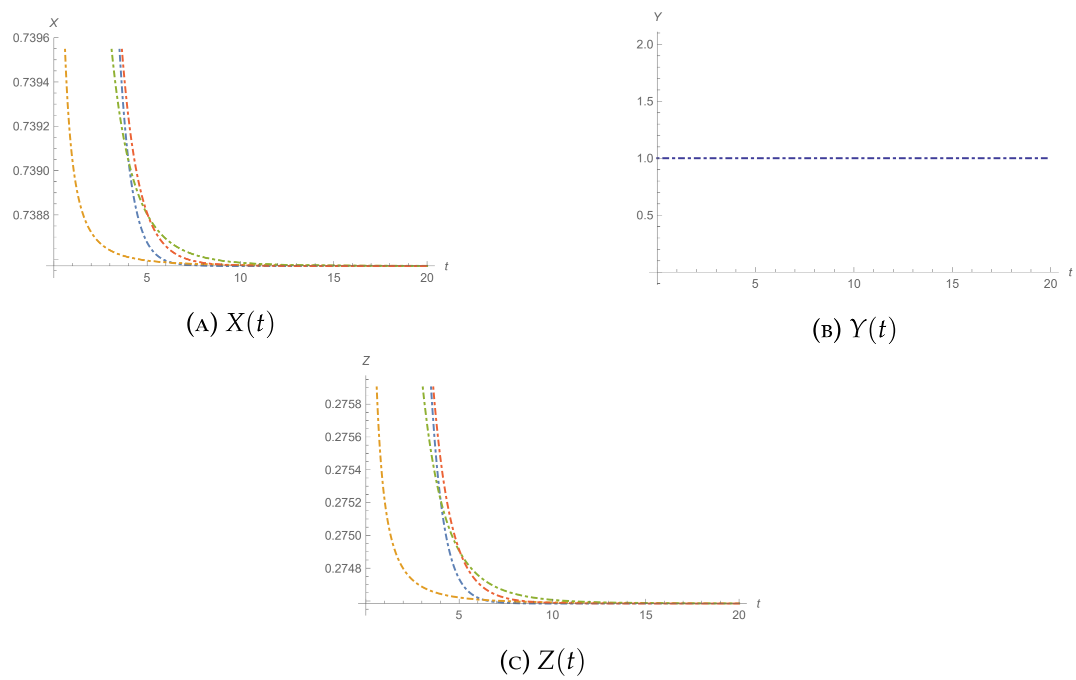

(A) $X(t)$ (B) $Y(t)$

(C) $Z(t)$

Figure 13. Asymptotic behavior of the agroecological system with μ_X, K_S, γ_X, and β_Z from H3YZdZ; μ_Y from H3YZdY0; and μ_Z and K_Z from H2XYdZ.

5. Results Discussion

First, we highlight the initial conditions used in all preceding visualizations, which serve as keys for clear interpretation and deeper understanding:

- For the initial condition (4.4), we set $X_0 = 1$.
- For the initial condition (4.7), we set $Y_0 = 1$.
- For the initial condition (4.10), we set $Z_0 = 1$.

In all figures, the colors represent the behavior of $X(t)$, $Y(t)$, or $Z(t)$ (as indicated on the axes) corresponding to different values of the fractional order α:

- Blue curve: Solution with integer order $\alpha = 1$.
- Yellow curve: Solution with fractional order $\alpha = \frac{1}{4}$.
- Green curve: Solution with fractional order $\alpha = \frac{1}{2}$.
- Red curve: Solution with fractional order $\alpha = \frac{3}{4}$.

Acknowledgment: The authors would like to express their sincere gratitude to the University of Jordan for its generous support through the funded research project (Project No. 782-1-2024), which greatly facilitated the successful completion of this work. Also, they would like to express their sincere gratitude to Ajman University for its support in facilitating the completion of this research.

Conflicts of Interest: The authors declare that there are no conflicts of interest regarding the publication of this paper.

References

[1] N.R. Anakira, A. Almalki, D. Katatbeh, G.B. Hani, A.F. Jameel, K.S. Al Kalbani, M. Abu-Dawas, An Algorithm for Solving Linear and Non-Linear Volterra Integro-Differential Equations, Int. J. Adv. Soft Comput. Appl. 15 (2023), 70–83.

[2] G. Farraj, B. Maayah, R. Khalil, W. Beghami, An Algorithm for Solving Fractional Differential Equations Using Conformable Optimized Decomposition Method, Int. J. Adv. Soft Comput. Appl. 15 (2023), 187–196.

[3] M. Berir, Analysis of the Effect of White Noise on the Halvorsen System of Variable-Order Fractional Derivatives Using a Novel Numerical Method, Int. J. Adv. Soft Comput. Appl. 16 (2024), 294–306.

[4] K.M. Dharmalingam, N. Jeeva, N. Ali, R.K. Al-Hamido, S.E. Fadugba, K. Malesela, F.T. Tolasa, H.S. El-Bahkiry, M. Qousini, Mathematical Analysis of Zika Virus Transmission: Exploring Semi-Analytical Solutions and Effective Controls, Commun. Math. Biol. Neurosci. 2024 (2024), 112. https://doi.org/10.28919/cmbn/8719.

[5] M. Aljazzazi, S. Fakhreddine, I. Batiha, I. Jebril, A. Bouchenak, et al., Impulsive Conformable Evolution Equations in Banach Spaces with Fractional Semigroup, Filomat 38 (2024), 9321–9332. https://doi.org/10.2298/fil2426321a.

[6] A. Al-nana, I.M. Batiha, I.H. Jebril, S. Alkhazaleh, T. Abdeljawad, Numerical Solution of Conformable Fractional Periodic Boundary Value Problems by Shifted Jacobi Method, Int. J. Math. Eng. Manag. Sci. 10 (2025), 189–206. https://doi.org/10.33889/ijmems.2025.10.1.011.

[7] A. Bouchenak, I.M. Batiha, R. Hatamleh, M. Aljazzazi, I.H. Jebril, et al., Study and Analysis of the Second Order Constant Coefficients and Cauchy-Euler Equations via Modified Conformable Operator, Int. J. Robot. Control. Syst. 5 (2025), 794–812. https://doi.org/10.31763/ijrcs.v5i2.1577.

[8] A. Bouchenak, I.M. Batiha, I.H. Jebril, M. Aljazzazi, H. Alkasasbeh, et al., Generalization of the Nonlinear Bernoulli Conformable Fractional Differential Equations with Applications, WSEAS Trans. Math. 24 (2025), 168–180. https://doi.org/10.37394/23206.2025.24.17.

[9] A. Bouchenak, I.M. Batiha, M. Aljazzazi, N. Anakira, M. Odeh, R.I. Hajaj, Numerical and Analytical Investigations of Fractional Self-Adjoint Equations and Fractional Sturm-Liouville Problems via Modified Conformable Operator, J. Robot. Control 6 (2025), 1410–1424.

[10] S. Fakhreddine, A.A. Hazaymeh, M. Aljazzazi, R. Qaralleh, A. Bataihah, I.M. Batiha, R.I. Hajaj, Analytical Investigation of the Existence and Ulam Stability of Integro-Differential Equations With Conformable Derivatives Under Non-Local Conditions, Int. J. Robot. Control Syst. 5 (2025), 1596–1607.

[11] M. Aljazzazi, F. Seddiki, I. Batiha, A. Bouchenak, R.I. Hajaj, Results on the Existence of Solutions for Conformable Evolution Differential Equations with Non-Local Conditions, Gulf J. Math. 20 (2025), 26–38. https://doi.org/10.56947/gjom.v20i2.3016.

[12] R. Khalil, M. Al Horani, A. Yousef, M. Sababheh, A New Definition of Fractional Derivative, J. Comput. Appl. Math. 264 (2014), 65–70. https://doi.org/10.1016/j.cam.2014.01.002.

[13] S. Kumar, R.S. Meena, R. Datta, S.K. Verma, G.S. Yadav, et al., Legumes for Carbon and Nitrogen Cycling: An Organic Approach, in: Carbon and Nitrogen Cycling in Soil, Springer Singapore, 2019: pp. 337–375. https://doi.org/10.1007/978-981-13-7264-3_10.

[14] R.L. Magin, Fractional Calculus in Bioengineering: A Tool to Model Complex Dynamics, in: Proceedings of the 13th International Carpathian Control Conference (ICCC), IEEE, 2012, pp. 464-469. https://doi.org/10.1109/carpathiancc.2012.6228688.

[15] H. Sun, Y. Zhang, D. Baleanu, W. Chen, Y. Chen, A New Collection of Real World Applications of Fractional Calculus in Science and Engineering, Commun. Nonlinear Sci. Numer. Simul. 64 (2018), 213–231. https://doi.org/10.1016/j.cnsns.2018.04.019.

[16] I. Podlubny, Fractional Differential Equations, Elsevier, Amsterdam, 1998.

[17] T. Crews, M. Peoples, Legume Versus Fertilizer Sources of Nitrogen: Ecological Tradeoffs and Human Needs, Agric. Ecosyst. Environ. 102 (2004), 279–297. https://doi.org/10.1016/j.agee.2003.09.018.

[18] V. Ajraldi, M. Pittavino, E. Venturino, Modeling Herd Behavior in Population Systems, Nonlinear Anal.: Real World Appl. 12 (2011), 2319–2338. https://doi.org/10.1016/j.nonrwa.2011.02.002.

[19] K. Louie, G.C. Wake, G. Lambert, A. MacKay, D. Barker, A Delay Model for the Growth of Ryegrass–Clover Mixtures: Formulation and Preliminary Simulations, Ecol. Model. 155 (2002), 31–42. https://doi.org/10.1016/s0304-3800(02)00063-7.

[20] K. Unami, Fractional Interpolation of the Unit-Hydrograph Method and the Lumped Flow Routing Method in Hydrology, in: 2023 International Conference on Fractional Differentiation and Its Applications (ICFDA), IEEE, 2023, pp. 1-4. https://doi.org/10.1109/icfda58234.2023.10153368.

[21] T. Abdeljawad, On Conformable Fractional Calculus, J. Comput. Appl. Math. 279 (2015), 57–66. https://doi.org/10.1016/j.cam.2014.10.016.

[22] M.B. Peoples, P.M. Chalk, M.J. Unkovich, R.M. Boddey, Can Differences in 15n Natural Abundance Be Used to Quantify the Transfer of Nitrogen From Legumes to Neighbouring Non-Legume Plant Species?, Soil Biol. Biochem. 87 (2015), 97–109. https://doi.org/10.1016/j.soilbio.2015.04.010.

[23] K.A. Jacot, A. Lüscher, J. Nösberger, U.A. Hartwig, Symbiotic N_2 Fixation of Various Legume Species Along an Altitudinal Gradient in the Swiss Alps, Soil Biol. Biochem. 32 (2000), 1043–1052. https://doi.org/10.1016/s0038-0717(00)00012-2.

[24] F.P. Vinther, E.S. Jensen, Estimating Legume N_2 Fixation in Grass-Clover Mixtures of a Grazed Organic Cropping System Using Two Methods, Agric. Ecosyst. Environ. 78 (2000), 139–147. https://doi.org/10.1016/s0167-8809(99)00124-3.

[25] E.C. Reilly, J.L. Gutknecht, N.E. Tautges, C.C. Sheaffer, J.M. Jungers, Nitrogen Transfer and Yield Effects of Legumes Intercropped with the Perennial Grain Crop Intermediate Wheatgrass, Field Crop. Res. 286 (2022), 108627. https://doi.org/10.1016/j.fcr.2022.108627.

[26] S. Das, P. Gupta, A Mathematical Model on Fractional Lotka–Volterra Equations, J. Theor. Biol. 277 (2011), 1–6. https://doi.org/10.1016/j.jtbi.2011.01.034.

[27] W. Guo, E.J. Magero, K. Unami, H. Shinjo, T. Izumi, A Dynamical System Model for Plant-Nutrient Interactions with Symbiotic Nitrogen Fixation and Allee Effect, Nonlinear Sci. 2 (2025), 100018. https://doi.org/10.1016/j.nls.2025.100018.

[28] T. Yoneyama, T. Omata, S. Nakata, J. Yazaki, Fractionation of Nitrogen Isotopes During the Uptake and Assimilation of Ammonia by Plants, Plant Cell Physiol. 32 (1991), 1211–1217. https://doi.org/10.1093/oxfordjournals.pcp.a078199.

[29] T. Yoneyama, K. Fujita, T. Yoshida, T. Matsumoto, I. Kambayashi, et al., Variation in Natural Abundance of 15n Among Plant Parts and in 15n/14n Fractionation During N2 Fixation in the Legume-Rhizobia Symbiotic System, Plant Cell Physiol. 27 (1986), 791–799. https://doi.org/10.1093/oxfordjournals.pcp.a077165.

[30] G. Mabaya, K. Unami, H. Yoshioka, J. Takeuchi, M. Fujihara, Robust Optimal Diversion of Agricultural Drainage Water From Tea Plantations to Paddy Fields During Rice Growing Seasons and Non-Rice Growing Seasons, Paddy Water Environ. 14 (2015), 247–258. https://doi.org/10.1007/s10333-015-0494-y.